🔓 **Open Access**

Multiple Microwave Frequency Measurement With Improved Resolution Based on Stimulated Brillouin Scattering and Nonlinear Fitting
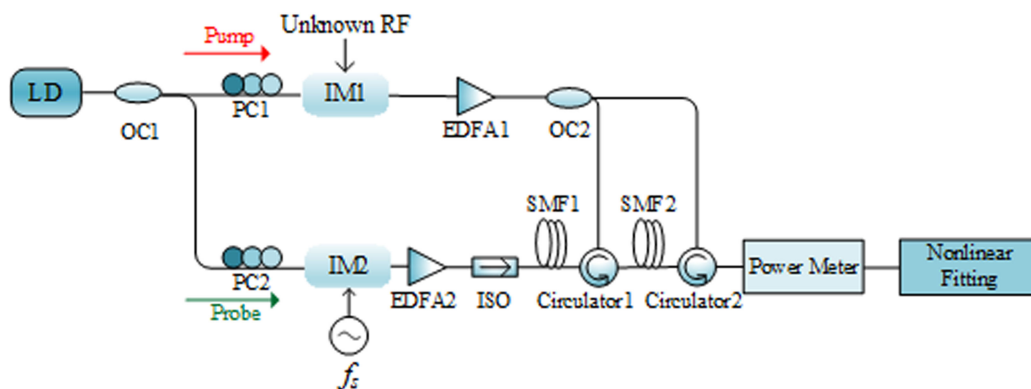
Wenting Jiao
Ke You
Junqiang Sun

Multiple Microwave Frequency Measurement With Improved Resolution Based on Stimulated Brillouin Scattering and Nonlinear Fitting

Wenting Jiao, Ke You, and Junqiang Sun (ORCID)

Wuhan National Laboratory for Optoelectronics, School of Optical and Electronic Information, Huazhong University of Science and Technology, Wuhan 430074, China

Abstract: A multiple microwave frequency measurement is experimentally demonstrated by exploiting stimulated Brillouin scattering and nonlinear fitting. Through sweeping a reference frequency during the stimulated Brillouin scattering process, the frequency information of microwave signal to be measured is detected by the created mapping between the total output power of the system and the reference frequency. Nonlinear fitting is utilized to mitigate the limitation of Brillouin gain spectrum linewidth and the measurement resolution is improved significantly. The minimum distinguishable frequency interval of 18 MHz is realized with the proposed scheme, and the measurement error is less than 5 MHz with in a range of 21.42 GHz. This approach offers an effective way to implement the measurement on continuous microwave sinusoidal signal with a number of frequencies of about 1190 in photonics domain.

Index Terms: Scattering, fiber non-linear optics, microwave photonics signal processing.

1. Introduction

Estimation of an unknown microwave signal, including its amplitude, phase and frequency, has vital applications in modern radar, high speed communications and space exploration fields [1]. Meanwhile, frequency measurement is mainly applied to antistealth defense, radar warning receivers and electronic intelligence systems. However, modern electrical microwave frequency measurement systems have a limited measurement range up to around 18 GHz [2]. In the past few years, photonic-assisted microwave frequency measurement (MFM) has drawn much attention for its advantages of large bandwidth, low loss, light weight, immunity to electromagnetic interference and large measurement range compared to electrical methods [3].

Recently, a great deal of photonic-assisted MFM schemes have been proposed based on birefringence effect [4], relative time delays [5], double mixing technique [6], the processing of an interferogram [7] and serial channelization [8], requiring highly nonlinear media, dispersive medium, high-speed optoelectronic devices, tunable photonic microwave notch filter and optical hybrid and balanced photodetectors. Besides, the scheme based on stimulated Brillouin scattering (SBS) is widely investigated [1]–[3], [9] since SBS is one of the most common nonlinear effects in single mode fiber. SBS process can be classically described as the nonlinear interaction between pump and
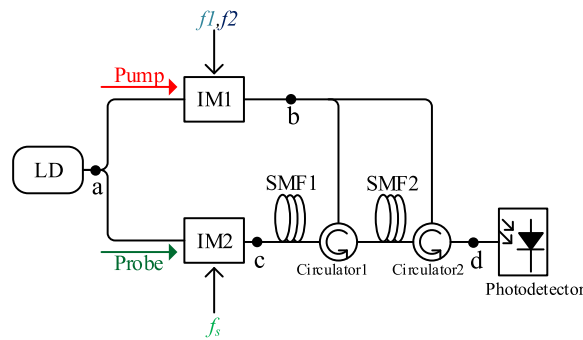
Fig. 1. Schematic diagram of the proposed MFM scheme. LD, laser diode; IM, Intensity modulator; SMF, single mode fiber.

Stokes waves through acoustic wave. A proportion of the pump energy is transferred to backward Stokes wave as long as the input pump power is higher than the SBS threshold. A Brillouin gain spectrum (BGS) centering on Stokes wavelength is generated. The Brillouin gain reaches its maximum when the frequency difference between input counter-propagating probe and pump waves equals Brillouin frequency shift (BFS). In [1], an instantaneous frequency measurement scheme based on SBS is presented. The system can detect several types of signals including linearly frequency modulated pulse and frequency Costas coded pulse with errors of 20 MHz. Reference [3] has broadened measurement range by applying two pumps to generate SBS through four modulators. In [9], a MFM scheme is proposed by exploiting the selective phase modulation to amplitude modulation conversion (PM-to-AM) realized through SBS. And the measurement is performed by a cymoscope and a digital oscilloscope at a 30-MHz measurement error. In [2], a centimeter-scale chalcogenide glass waveguide is used to generate SBS to build power-to-frequency mappings and amplitude comparison function (ACF) in different frequency bands. The system in [2] achieves a large measurement range up to 38 GHz with a 1-MHz error, however, at the expense of high cost and increased complexity of the system. As multiple microwave frequencies need to be measured, the frequency resolution is largely limited by the BGS linewidth. Narrower BGS linewidth is helpful to distinguish smaller frequency difference. The BGS linewidth is usually considered to be 30 MHz in single mode fiber (SMF) [1] and significant reduction of the linewidth commonly comes at the cost of increasing the complexity of the system [10]–[13]. In [12], a dual-stage SBS structure is presented owing to its narrower BGS linewidth compared with single stage structure, and an experiment is carried out to prove the important role of dual-stage SBS structure in enhancing the storage time of the aquasi-light storage system.

In this paper, a simple and feasible multiple MFM scheme utilizing dual-stage SBS and nonlinear fitting is proposed and experimentally demonstrated. Unknown multiple frequencies that are required to be discriminated and the reference frequency signal are modulated onto the carrier wave respectively, both involving in the nonlinear SBS interaction. By monitoring the changes of the output optical power of the system along with the sweeping reference frequency, the unknown multiple microwave frequencies can be evaluated without ACF. Dual-stage SBS structure is introduced to the proposed system to achieve measurements with low error. Since the competence of the dual-stage structure to improve the frequency resolution is insufficient, nonlinear fitting method is applied to the measured data processing. The frequency resolution of the system is mainly reduced by nonlinear fitting. The minimum resolvable frequency difference of 18 MHz is realized when multiple frequencies are measured. The measurement error is less than 5 MHz with a broadband of 21.42 GHz.

2. Operational Principle

The schematic diagram of the proposed MFM scheme is shown in Fig. 1. The optical carrier from laser diode (LD) is coupled into two paths, acting as pump and probe wave separately. In the
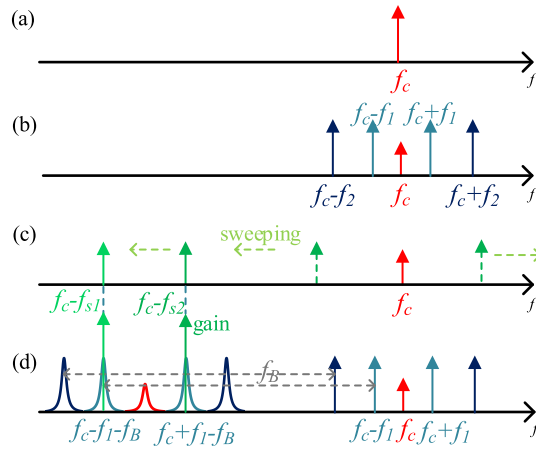
Fig. 2. The frequency relationships corresponding to different points in Fig. 1.

upper path, the pump wave is modulated by the radio frequency (RF) signal with multiple unknown frequencies. One, two or more frequencies can be measured through the proposed scheme, as illustrated in Fig. 1 with two frequencies (f_1, f_2). This modulated pump wave is separately fed into two segments of SMF with same BFS by two circulator to generate dual-stage SBS. The dual-stage pump configuration is employed in the proposed scheme to achieve lower measurement error than the single stage pump system, as the decrease of the BGS linewidth is accompanied by the decrease of the measurement error. In the lower path, the reference frequency signal (f_s) is modulated onto the probe wave. This modulated probe wave enters the two SMF and is power-affected by the generated SBS gain. The photodetector is used to monitor the total output optical power of the system.

Fig. 2(a)–(d) show the frequency relationships at several significant points in the upper schematic diagram. Here f_c represents the optical carrier frequency. f_1 and f_2, assumed the unknown microwave frequencies, are double sideband modulated onto the pump wave via an intensity modulator (IM), shown in Fig. 2(b). As pump power higher than the SBS threshold travels along SMF, Brillouin scattering will be generated and each sideband within the pump wave will create a corresponding Brillouin gain spectrum. The center of the BGS differs from the pump wave by a BFS (f_B). The Brillouin gain can be expressed as

$$g(f) = g_0 \frac{\left(\frac{\Delta v_B}{2}\right)^2}{f^2 + \left(\frac{\Delta v_B}{2}\right)^2} \tag{1}$$

Where g_0 is the peak Brillouin gain, Δv_B is the Brillouin linewidth. f represents the frequency offset to the Brillouin gain peak.

The reference frequency f_s is also double sideband modulated onto the optical carrier wave, shown in Fig. 2(c). During the measurements, the reference frequency sweeps with a certain frequency interval. As f_s sweeps, the output optical power will be influenced by f_s owing to the SBS effect. Only the total output optical power of the system needs to be monitored and a mapping between the output optical power and f_s is formed. The total output power of the system will reach its maximum value when the frequency of the sideband of the modulated probe wave, $f_c - f_{s1}$ ($f_c - f_{s2}$), is equal to the central frequency of the BGS, $f_c - f_1 - f_B$ ($f_c + f_1 - f_B$). f_{s1} and f_{s2} represent two values of sweeping reference frequency. As a result, the unknown microwave frequency f_1 can be determined by the expression $f_{s1} - f_B$ ($f_B - f_{s2}$). Two measuring results for one frequency will be observed because of the symmetry of the double sideband modulated pump signal. Other microwave frequencies, for instance f_2, are measured in the same way as f_1. Fig. 3 shows optical spectra of the pump wave and probe wave for three RF signals with different frequency ranges,
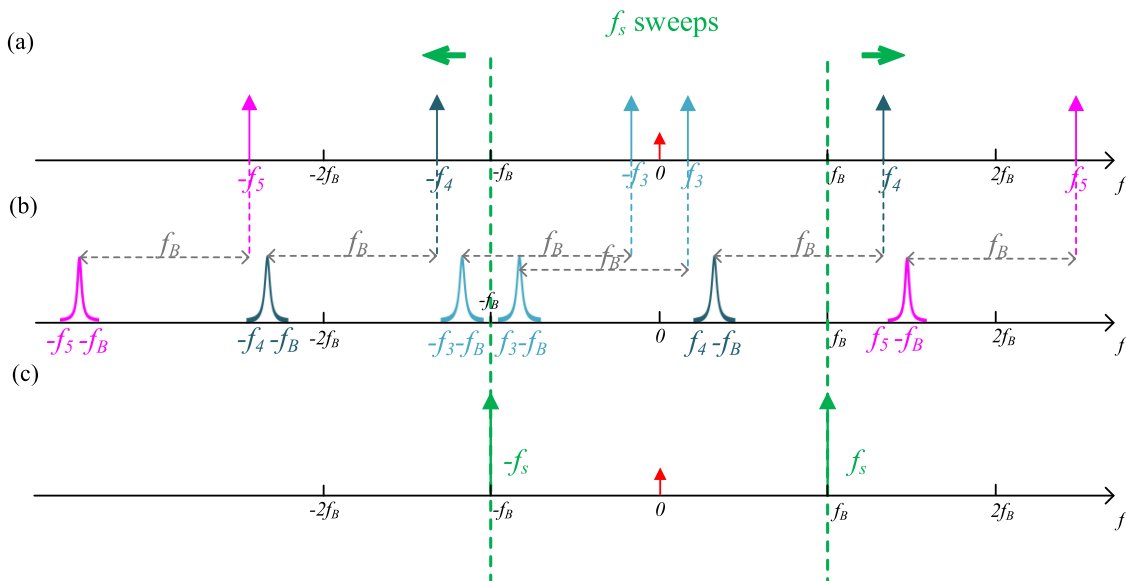
Fig. 3. Optical spectra for the RF signals of different frequencies, $f_3 < f_B$, $f_B < f_4 < 2f_B$, $f_5 > 2f_B$. (a) RF signals are modulated to the pump wave; (b) BGS generated by the modulated pump wave; (c) the reference frequency f_s is modulated to the probe wave and starts scanning from f_B.

$f_3 < f_B$, $f_B < f_4 < 2f_B$, $f_5 > 2f_B$. If f_s scans from zero, both the upper and lower sidebands of f_s are magnified by the BGS generated by the modulated pump wave, displayed in Fig. 3(b) and (c). Then the photodetector will detect many power peaks but cannot judge whether they come from the upper or lower band amplification of f_s, resulting in ambiguity of measurement. It can be seen from Fig. 3(b) that the BGS produced by the pump wave is symmetrically distributed centered on $-f_B$. If f_s starts sweeping from f_B, the lower sideband of f_s will sweep through the BGS (centering on $-f_3 - f_B$, $-f_4 - f_B$, and $-f_5 - f_B$) produced by the lower sideband of the modulated pump light from -f_B without missing, and the upper sideband of f_s will not be enlarged by any BGS as long as the frequencies of the RF signals are all less than $2f_B$. Therefore, the double-sideband modulated f_s, sweeping from f_B, can actualize the measurement without ambiguity in the range of $2f_B$ in common with single sideband modulation. Double sideband modulation is easier to implement, more practical and is capable of accurate measurement in the range of not less than 20 GHz (the f_B of SMF is generally 10 GHz).

Multiple frequencies can be measured simultaneously when the frequencies of the signals remain constant for a period of time or during one sweeping cycle of the reference frequency. If the frequencies of the signals are variable, the change of the frequencies can still be captured as long as the time interval for change is larger than a sweeping cycle of the reference frequency. The number of the monitored power peaks after one sweeping cycle of the reference frequency is the number of the unknown frequencies. Whether in our scheme or other SBS-based MFM schemes, BFS is a so significant parameter that needs to be accurately measured. In our scheme, BFS can be expediently measured with RF signal by controlling the bias voltage of IM1. The carrier of the modulated pump wave can also generate a BGS and BFS can be evaluated by $f_c - f_s = f_c - f_B$ in the same way as RF signal mentioned above, since the bias voltage of IM1 is adjusted to an appropriate value. In addition, the bias voltage needs to be controlled within the linear modulation range to avoid harmonics. The existence of harmonics may lead to the misjudgment of frequency. It is hardly necessary to precisely control the bias voltage of IM, provided that the intensities of the sidebands are large enough to produce SBS.

The minimum distinguishable frequency difference is an important parameter in MFM system. When the frequency difference between f_1 and f_2 is so small that their generated BGS overlap

significantly, the two frequencies cannot be discriminated efficiently by sweeping the reference frequency. The smaller the frequency difference is, the larger the overlap area of the generated two BGS will be, leading to more difficult to distinguish two frequencies. To identify two frequencies with smaller frequency difference, nonlinear fitting is applied to the proposed system.

Given n data points (x_i, y_i) $(i = 1, 2 \ldots n)$ with nonlinear relations, nonlinear fitting is to find a function $F(\mathbf{P}, x)$ that is closest to all data points under a certain criterion. Having simple calculation and extensive application, the least squares criterion is to minimize the sum of the squared distances from all the points to the function $F(\mathbf{P}, x)$. The sum of the squared distances is expressed as follows [14]

$$d = \sum_{i=1}^{n} [F(\mathbf{P}, x) - y_i]^2 \qquad \mathbf{P} = (p_1, p_2, \ldots, p_m)^T \tag{2}$$

Where p_j $(j = 1, 2 \ldots m)$ are the fitting parameters to be calculated and m is smaller than n. The condition for d to be a minimum is that the partial derivatives of d with respect to p_j are all equal to zero, written as

$$\begin{cases} L_1(p) = \frac{\partial d}{\partial p_1} = 2 \sum_{i=1}^{n} [F(\mathbf{P}, x) - y_i] \frac{\partial F(\mathbf{P}, x)}{\partial p_1} = 0 \\ L_2(p) = \frac{\partial d}{\partial p_2} = 2 \sum_{i=1}^{n} [F(\mathbf{P}, x) - y_i] \frac{\partial F(\mathbf{P}, x)}{\partial p_2} = 0 \\ \ldots \\ L_m(p) = \frac{\partial d}{\partial p_m} = 2 \sum_{i=1}^{n} [F(\mathbf{P}, x) - y_i] \frac{\partial F(\mathbf{P}, x)}{\partial p_m} = 0 \end{cases} \tag{3}$$

The problem is transformed into solving the following nonlinear equation

$$\mathbf{L}(\mathbf{P}) = \mathbf{0} \qquad \mathbf{L} = (L_1, L_2, \ldots, L_m)^T \tag{4}$$

The Levenberg-Marquardt method are employed to solve the above nonlinear equations. The iterative calculation formula of Levenberg-Marquardt method is [15]

$$\mathbf{P}^{(k+1)} = \mathbf{P}^{(k)} - \left(\mathbf{J}_L^T \mathbf{J}_L + \lambda \mathbf{I}\right)^{-1} \mathbf{J}_L^T \mathbf{L}\left(\mathbf{P}^{(k)}\right) \qquad k = 0, 1, 2, \ldots \tag{5}$$

$$\mathbf{J}_L = \begin{bmatrix} \frac{\partial L_1}{\partial p_1} & \frac{\partial L_1}{\partial p_2} & \cdots & \frac{\partial L_1}{\partial p_m} \\ \frac{\partial L_2}{\partial p_1} & \frac{\partial L_2}{\partial p_2} & \cdots & \frac{\partial L_2}{\partial p_m} \\ \vdots & \vdots & \ddots & \vdots \\ \frac{\partial L_m}{\partial p_1} & \frac{\partial L_m}{\partial p_2} & \cdots & \frac{\partial L_m}{\partial p_m} \end{bmatrix} \tag{6}$$

Where $\mathbf{J}_L$ is the Jacobian matrix of the nonlinear equation $\mathbf{L}(\mathbf{P})$ and $\mathbf{I}$ represents the identity matrix, λ is the damping parameter. The damping parameter influences the descent speed of the equation $\mathbf{L}(\mathbf{P})$ and its value will be adjusted according to the distance between the current iteration and the solution of the expression (4). After a large number of iterative calculations, $\mathbf{P}^{(k+1)}$ in expression (5) will be eventually approachable to the solution of the equations in an acceptable precision. The Levenberg-Marquardt method has a high speed of convergence and low dependence on initial value $\mathbf{P}^{(0)}$. The iteration computing process can be conveniently actualized by programming.

Based on the Lorentz line type of BGS profile governed by expression (1), the function can be written as

$$F(\mathbf{P}, x) = \frac{p_1}{(x - p_2)^2 + p_3} + \frac{p_4}{(x - p_5)^2 + p_6} + p_7 \tag{7}$$

p_2 and p_5 are the central frequencies of the two overlapped BGS. p_3 and p_6 represents the square of half the Brillouin linewidth. p_1 (p_4) is equal to the product of peak Brillouin gain and p_3 (p_6). p_7 is
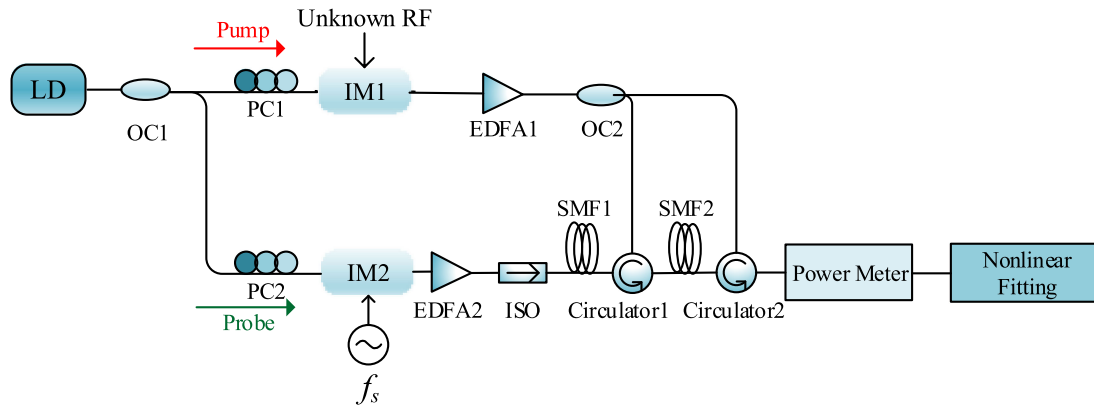
Fig. 4. Experimental setup for the proposed MFM scheme. LD: laser diode; OC: optical coupler; PC: polarization controller; IM: intensity modulator; EDFA: erbium-doped fiber amplifier; ISO: isolator; SMF: single mode fiber.

a constant. Each parameter has an initial value and the fitting program will give the final parameter values after a lot of iterative calculations. The initial values can be confirmed by following formulas

$$\mathbf{P}^{(0)} = \left(p_1^{(0)}, p_2^{(0)}, \dots, p_7^{(0)}\right)^T \tag{8}$$

$$p_2^{(0)} = p_5^{(0)} = x^{max} \tag{9}$$

$$p_3^{(0)} = p_6^{(0)} = \left(\frac{\Delta \nu_B}{2}\right)^2 \tag{10}$$

$$p_1^{(0)} = p_4^{(0)} = \frac{1}{2}\left(y_{max} - y_{min}\right)p_3^{(0)} \tag{11}$$

$$p_7^{(0)} = y_{min} \tag{12}$$

Where y_{max} and y_{min} are the maximum and minimum values of $y_i (i = 1, 2 \dots n)$ respectively, x^{max} is the data corresponding to y_{max} at (x^{max}, y_{max}). Small deviations of initial values will not have much impact on the final iteration results. By utilizing this data fitting method, the minimum distinguishable frequency difference of the proposed system can be significantly reduced.

3. Experimental Setup and Results

The experimental setup for the proposed MFM system based on SBS is depicted in Fig. 4. The laser coming out from a tunable laser diode (LD, APEX AP3350A) with a 3-MHz spectrum linewidth is launched into two paths by a 3 dB optical coupler (OC). Both paths of the light go through a polarization controller (PC1 or PC2) to get an optimized polarization state, since SBS is polarization sensitive. The modulation is actualized by two intensity modulators (IM1 and IM2, iXblue MXAN-LN-40 and Optilab IM-1550-40-PM-HER) with 40-GHz modulation bandwidth. In the process of measuring the unknown frequencies, the bias voltage of IM1 is set at about 10 V. We assume the RF signal comprises one, two or multiple unknown frequencies. Erbium-doped fiber amplifiers (EDFA1 and EDFA2) are used to compensate the optical transmission loss and control the pump and probe power individually. Then the modulated pump wave is coupled into two branches by another OC. The pump waves within two branches come into two segments of 2-km SMF by two circulators to generate dual-stage SBS. An isolator (ISO) is utilized to block the residual pump light after SBS and avoid damage to the active device front. The total output optical power of the system is monitored by a power meter with a resolution of 0.01 dB.
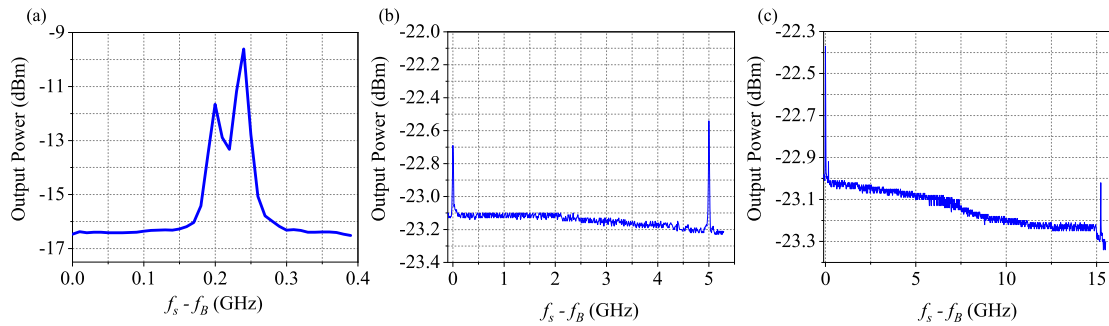
Fig. 5. Measured total output power against $f_s - f_B$ for three groups of RF signals. (a) 0.2 GHz and 0.24 GHz; (b) 5 GHz; (c) 15.23 GHz.
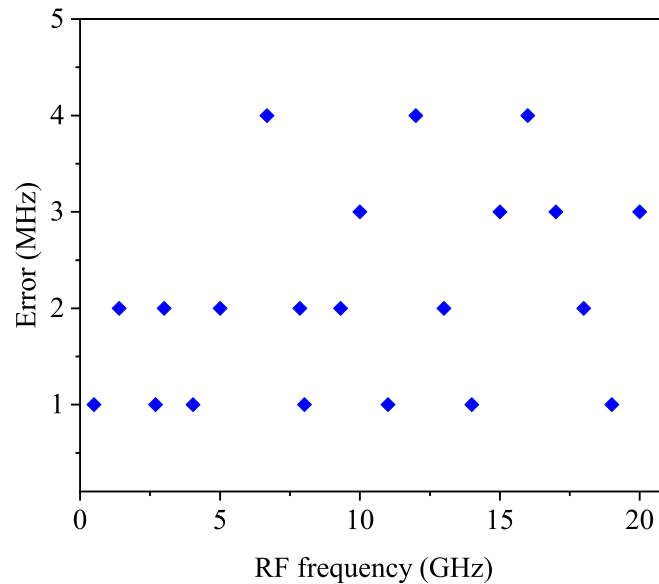

Fig. 6. The variations of measured errors with the RF frequency.

Fig. 5 shows the measured mapping of the total output power against $f_s - f_B$ for three groups of RF signals where f_B is measured to be 10.71 GHz. The reference frequency f_s sweeps at a step size of 1 MHz. The frequencies of the three sets of RF signals are 0.2 GHz and 0.24 GHz, 5 GHz, 15.23 GHz with the pump power of 17.30 dBm, 17.28 dBm and 17.25 dBm respectively to generate SBS. The values of $f_s - f_B$ corresponding to each peak power in Fig. 5 are the measured frequencies, 0.2 GHz and 0.24 GHz, 5 GHz, 15.23 GHz. Each local power maximum corresponds to a RF frequency. It is found from Fig. 5(b) and (c) that there is a local power maximum at $f_s - f_B = 0$, corresponding to the BGS generated by the optical carrier. The measurement range of the system is 21.42 GHz.

Fig. 6 illustrates the experimental errors when only one microwave frequency is measured. Owing to the restriction of experimental conditions, only the measurement errors for microwave frequency ranging from 0.1 GHz to 20 GHz (randomly selected frequencies) is obtained in the experiments. It indicates that the measurement errors are all less than 5 MHz. With the increment of the microwave frequency, the increasing tendency of the measured errors emerges, which mainly arises from the signal generator instability for the larger frequency.

To observe the minimum distinguishable frequency difference of the system, the mapping of the output power under different frequency differences is performed. Fig. 7(a)–(c) illustrate the mapping of the output power with $f_s - f_B$ when the frequencies of RF signals are 0.2 GHz and 0.24 GHz,
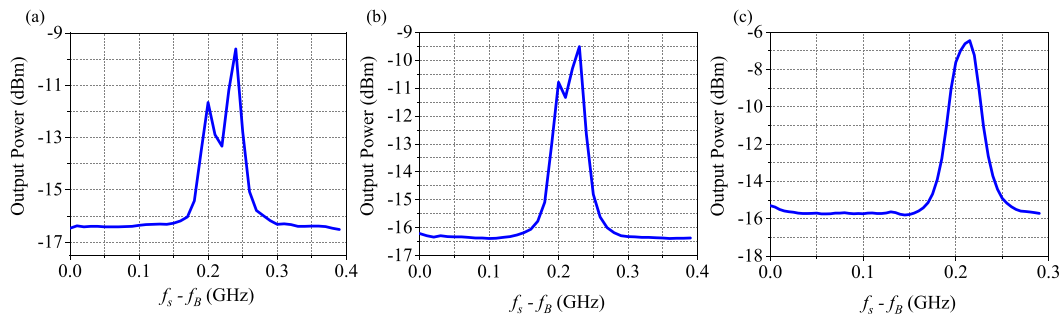
Fig. 7. Measured total output power against $f_s - f_B$ for three groups of RF signals. (a) 0.2 GHz + 0.24 GHz; (b) 0.2 GHz + 0.23 GHz; (c) 0.2 GHz + 0.22 GHz.

TABLE 1

The Fitting Results With Different Frequency Differences

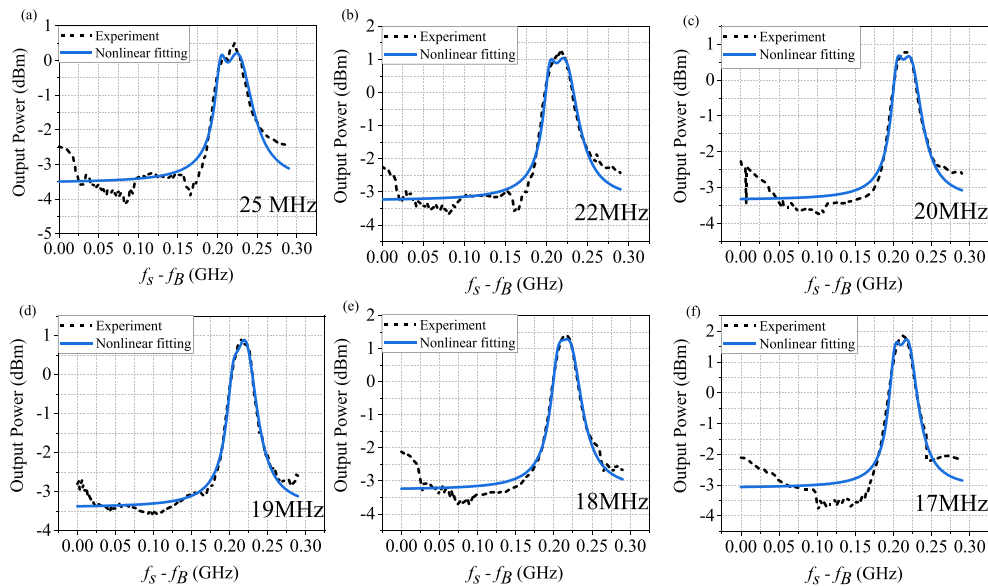| Difference (MHz)	f_1 (GHz)	p_2 (GHz)	Error1 (MHz)	f_2 (GHz)	p_5 (GHz)	Error2 (MHz)
25	0.2	0.2039	3.9	0.225	0.2260	1
22	0.2	0.2038	3.8	0.222	0.2227	0.7
20	0.2	0.2048	4.8	0.220	0.2229	2.9
19	0.2	0.2044	4.4	0.219	0.2214	2.4
18	0.2	0.2049	4.9	0.218	0.2218	3.8

Fig. 8. Nonlinear fitting results of experimental values for different frequency differences. (a) 25 MHz; (b) 22 MHz; (c) 20 MHz; (d) 19 MHz; (e) 18 MHz; (f) 17 MHz.

0.2 GHz and 0.23 GHz, 0.2 GHz and 0.22 GHz. The two frequencies can be clearly distinguished and measured when the frequency difference is 40 MHz in Fig. 7(a) and faintly discriminated when the frequency difference is reduced to 30 MHz in Fig. 7(b). As the frequency difference is set less than 20 MHz, the two power peaks are superimposed and completely indistinguishable. It can be deduced that the minimum distinguishable frequency difference of the system is about 30 MHz without nonlinear fitting.
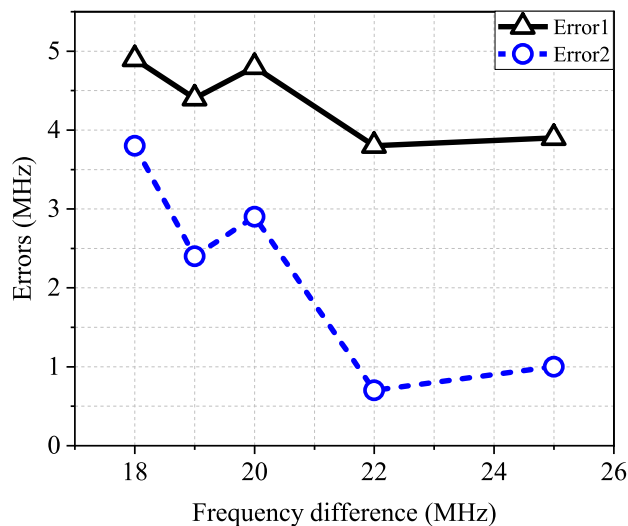
Fig. 9. Measured errors of two frequencies against different frequency differences.
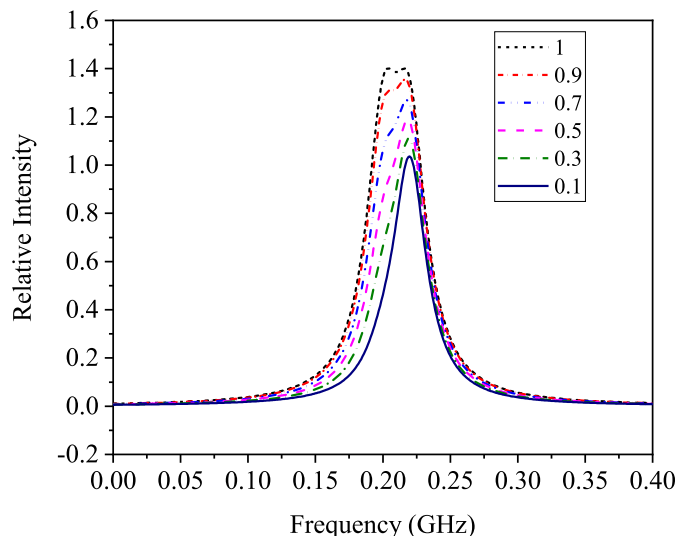

Fig. 10. Simulation results of the two frequencies with different power ratios when the two frequencies are 0.2 GHz and 0.22 GHz. The frequency difference is 20 MHz.

In order to measure the microwave frequencies with the frequency difference less than 30 MHz, nonlinear fitting is introduced in dealing with the mapping of the output optical power. The microwave frequencies and their corresponding fitting results with errors are exhibited in Table 1. p_2 and p_5 are parameters in expression (7) and represent the fitting values of f_1 and f_2 respectively. Fig. 8 shows the results of nonlinear fitting with different frequency differences lower than 30 MHz. The effect of nonlinear fitting is preferable near the power peaks. As the frequency difference is less than 18 MHz, the result of nonlinear fitting is not satisfactory.

Fig. 9 visually displays the measured errors after nonlinear fitting. It is noticed that all errors are lower than 5 MHz and the overall trend decreases with the increase of frequency difference. The measurement error of the frequency difference of 19 MHz is lower than that of 20 MHz potentially because of the instability of the experimental equipment. The lower one of the two frequencies has a larger error than the higher one, which can be ascribed to peak power difference between the frequencies. The small peak power corresponding to the lower frequency is more susceptible to

TABLE 2
The Fitting Results With Different Power Ratios

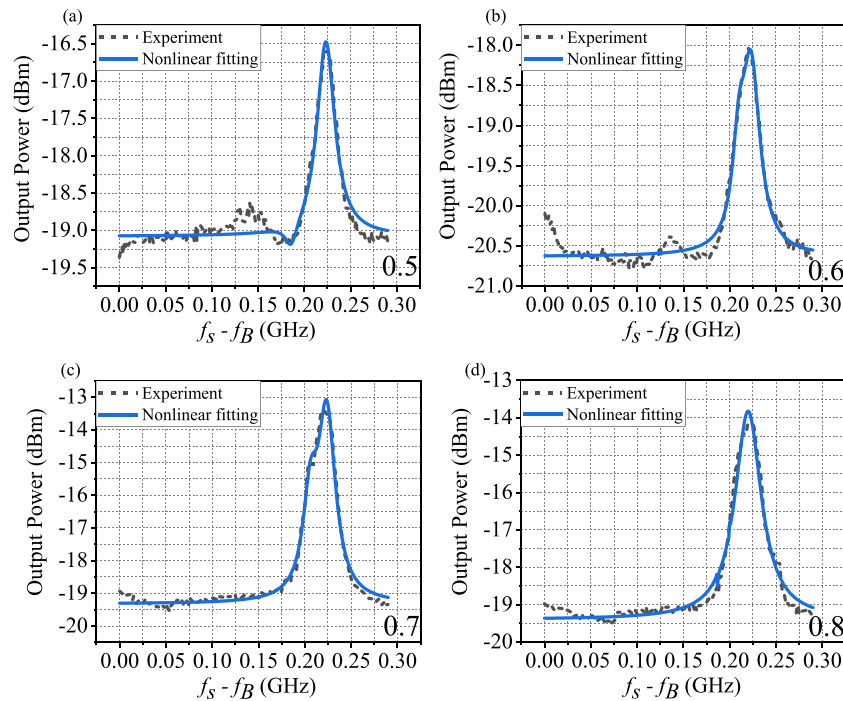| Power Ratio	f_1 (GHz)	p_2 (GHz)	Error3 (MHz)	f_2 (GHz)	p_5 (GHz)	Error4 (MHz)
0.5	0.2	0.1859	14.1	0.22	0.2233	3.3
0.6	0.2	0.2101	10.1	0.22	0.2233	3.3
0.7	0.2	0.2061	6.1	0.22	0.2238	3.8
0.8	0.2	0.1933	6.7	0.22	0.2200	0

Fig. 11. Nonlinear fitting results of the two RF signals with different power ratios and the frequency difference is 20 MHz. The power ratio is (a) 0.5; (b) 0.6; (c) 0.7; (d) 0.8.

the overlap than the large peak power of the higher frequency. After nonlinear fitting, the minimum distinguishable frequency difference has been reduced from 30 MHz to 18 MHz with measurement errors of 5 MHz.

From the above discussion, the measurement errors are different for different peak powers of the two frequencies. Thus, the influence of the optical power ratio of the two frequencies on the nonlinear fitting needs to be verified. The power ratio here is defined as the ratio of the optical power of the lower frequency to the higher frequency in the two-frequency measurement. Fig. 10 shows the numerical simulations of the power peak overlaps under different values of power ratio with the fixed frequency difference of 20 MHz. During the simulations, the peak power of the higher frequency is kept constant while the peak power of the lower frequency decreases. Thus, the optical power ratio is varied from 1 to 0.1.

With the decrease of the power ratio in Fig. 10, the smaller peak corresponding to the lower frequency will gradually submerge into the higher peak corresponding to the higher frequency and finally completely become invisible, resulting in a larger error of the lower frequency. The measurement experiments for two microwave frequencies, 0.2 GHz and 0.22 GHz, are performed with different power ratios selected to be 0.5, 0.6, 0.7 and 0.8. The nonlinear fitting results are listed
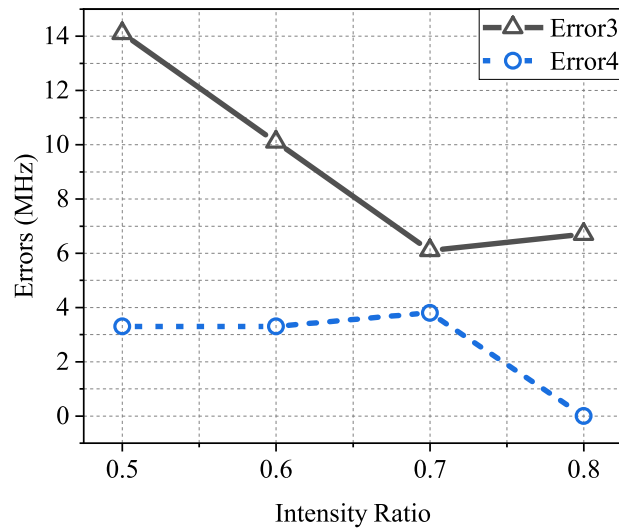
Fig. 12. Measured errors of the two frequencies with different power ratios after nonlinear fitting.

in Table 2 and illustrated in Fig. 11. It indicates that by taking into account the peak power difference between the frequencies, the nonlinear fitting for the experimental results will be impacted.

The errors after nonlinear fitting under different power ratios are graphically displayed in Fig. 12. Compared to the situation without considering the peak power difference, the errors of the lower frequency are slightly large. It is clear that the errors of the lower frequency are larger than that of the higher frequency. The measured errors of the higher frequency are all less than 5 MHz. Thus, we can conclude that the measurement errors decrease with the increase of the optical power ratio because it is easier to distinguish two frequencies with a larger optical power ratio.

4. Conclusion

A multiple MFM system with improved resolution is proposed and experimentally demonstrated based on SBS and nonlinear fitting. The Brillouin gain generated by the unknown microwave frequencies modulated pump light influences the counter-propagating probe light modulated by the reference frequency. The unknown microwave frequencies can be measured by monitoring the changes of the output optical power with the reference frequency. The dual-stage pump structure is applied to the system with the benefit of a narrower BGS linewidth compared with single stage pump structure. Through introducing the nonlinear fitting for the experimental results, the frequency discrimination limitation originating from the BGS linewidth is alleviated. Thus the minimum distinguishable frequency difference is reduced from 30 MHz to 18 MHz. A measurement error less than 5 MHz within a broadband of 21.42 GHz is realized when the distinguishable minimum frequency difference is 18 MHz. No ACF is utilized in the microwave frequency measurement system. The proposed approach can be broadened to more than dual-frequency measurement in photonics domain.

References

[1] X. Long, W. Zou, and J. Chen, "Broadband instantaneous frequency measurement based on stimulated Brillouin scattering," *Opt. Exp.*, vol. 25, pp. 2206–2214, 2017.
[2] H. Jiang *et al.*, "Wide-range, high-precision multiple microwave frequency measurement using a chip-based photonic Brillouin filter," *Optica*, vol. 3, pp. 30–34, 2016.
[3] Y. Xiao *et al.*, "Multiple microwave frequencies measurement based on stimulated Brillouin scattering with improved measurement range," *Opt. Exp.*, vol. 21, pp. 31740–31750, 2013.

[4] D. Feng, H. Xie, L. Qian, Q. Bai, and J. Sun, "Photonic approach for microwave frequency measurement with adjustable measurement range and resolution using birefringence effect in highly non-linear fiber," *Opt. Exp.*, vol. 23, pp. 17613–17621, 2015.

[5] Linh V. T. Nguyen, "Microwave photonic technique for frequency measurement of simultaneous signals," *IEEE Photon. Technol. Lett.*, vol. 21, no. 10, pp. 642–644, May 2009.

[6] H. Emami, N. Sarkhosh, and M. Ashourian, "Photonic simultaneous frequency identification of radio-frequency signals with multiple tones," *Appl. Opt.*, vol. 52, pp. 5508–5515, 2013.

[7] B. Vidal, T. Mengual, and J. Marti, "Photonic technique for the measurement of frequency and power of multiple microwave signals," *IEEE Trans. Microw. Theory Techn.*, vol. 58, no. 11, pp. 3103–3108, Nov. 2010.

[8] H.Chen, R. Li, C. Lei, Y. Yu, M. Chen, S. Yang, S. Xie, "Photonics-assisted serial channelized radio-frequency measurement system with nyquist-bandwidth detection," *IEEE Photon. J.*, vol. 6, no. 6, pp. 1–7, Dec. 2014.

[9] S. Zheng, S. Ge, X. Zhang, H. Chi, and X. Jin, "High-resolution multiple microwave frequency measurement based on stimulated brillouin scattering," *IEEE Photon. Technol. Lett.*, vol. 24, no. 13, pp. 1115–1117, Jul. 2012.

[10] S. Preussler and T. Schneider, "Stimulated Brillouin scattering gain bandwidth reduction and applications in microwave photonics and optical signal processing," *Opt. Eng.*, vol. 55, 2015, Art. no. 031110.

[11] A. Wiatrek, S. Preussler, K. Jamshidi, and T. Schneider, "Frequency domain aperture for the gain bandwidth reduction of stimulated Brillouin scattering," *Opt. Lett.*, vol. 37, pp. 930–932, 2012.

[12] S. Preussler and T. Schneider, "Bandwidth reduction in a multistage Brillouin system," *Opt. Lett.*, vol. 37, pp. 4122–4124, 2012.

[13] S. Preussler, A. Wiatrek, K. Jamshidi, and T. Schneider, "Brillouin scattering gain bandwidth reduction down to 3.4 MHz," *Opt. Exp.*, vol. 19, pp. 8565–8570, 2011.

[14] P. C. Hansen, V. Pereyra, and G. Scherer, "Nonlinear least squares problems," 2004.

[15] K. Madsen, H. B. Nielsen, and O. Tingleff, "Methods for non-linear least squares problems," 2nd ed. Informat. Math. Model., Tech. Univ. Denmark, Lyngby, Denmark, 2004.